Crystal Structure and Physicochemical Characterization of Ambazone Monohydrate, Anhydrous, and Acetate Salt Solvate

MARIETA MURESAN-POP,[1] DARIO BRAGA,[2] MIHAELA M. POP,[1] GHEORGHE BORODI,[1] IRINA KACSO,[1] LUCIA MAINI[2]

[1]National Institute for Research and Development of Isotopic and Molecular Technologies, Cluj-Napoca R-400293, Romania
[2]Dipartimento di Chimica G. Ciamician, Università di Bologna 40 126, Bologna, Italy

Received 10 April 2014; revised 7 August 2014; accepted 11 August 2014

Published online 3 September 2014 in Wiley Online Library (wileyonlinelibrary.com). DOI 10.1002/jps.24151

ABSTRACT: The crystal structures of the monohydrate and anhydrous forms of ambazone were determined by single-crystal X-ray diffraction (SC-XRD). Ambazone monohydrate is characterized by an infinite three-dimensional network involving the water molecules, whereas anhydrous ambazone forms a two-dimensional network via hydrogen bonds. The reversible transformation between the monohydrate and anhydrous forms of ambazone was evidenced by thermal analysis, temperature-dependent X-ray powder diffraction and accelerated stability at elevated temperature, and relative humidity (RH). Additionally, a novel ambazone acetate salt solvate form was obtained and its nature was elucidated by SC-XRD. Powder dissolution measurements revealed a substantial solubility and dissolution rate improvement of acetate salt solvated form in water and physiological media compared with ambazone forms. Also, the acetate salt solvate displayed good thermal and solution stability but it transformed to the monohydrate on storage at elevated temperature and RH. Our study shows that despite the requirement for controlled storage conditions, the acetate salt solvated form could be an alternative to ambazone when solubility and bioavailability improvement is critical for the clinical efficacy of the drug product. © 2014 Wiley Periodicals, Inc. and the American Pharmacists Association J Pharm Sci 103:3594–3601, 2014

Keywords: ambazone; antimicrobial; X-ray diffractometry; crystal structure; polymorphism; acetate salt solvate; proton transfer; dissolution rate; stability

INTRODUCTION

Poor physicochemical properties of pharmaceutical compounds can be improved by obtaining different crystalline forms including polymorphs, hydrates, salts, and cocrystals of active pharmaceutical ingredients (APIs). Salts of APIs are used when the API is not sufficiently soluble or stable due to the fact that different salt forms may have different profiles, or bioavailability properties.[1–4]

Ambazone, [4-(2-(diaminomethylidene) hydrazinyl)phenyl] iminothiourea or (*p*-benzoquinone amidinohydrazone thiosemicarbazone), is the active ingredient of Faringosept,[5] an antiseptic for the oral cavity because it is active in a number of pathogens that trigger infections of the mouth and upper respiratory tract. Moreover, ambazone has been used for a long time as a medicine for bacteriostatic activity, allowing the replacement of antibiotics in topical treatment of oral pharyngeal infections.[6–11] Further studies showed a possible anticancer activity of ambazone because of the amidinohydrazone group being an anticancer agent.[12,13] The commercial form of ambazone used in the pharmaceutical industry is the monohydrate form, which is slightly soluble in water and has a variable 35%–50% oral bioavailability affecting the therapeutic effect of the Faringosept tablets.

The molecular structure of ambazone (Fig. 1) is characterized by a thiosemicarbazone group and an amidinohydrazone group, these two groups allow the existence of several tautomers, and two of those are shown in Figure 1. Only one conformation of the thiosemicarbazone group is observed in the crystal structures reported in the Cambridge Structure Database (CSD), whereas two different tautomers are observed for the amidinohydrazone group. The hydrogen position of amidinohydrazone group in tautomer A (which is commonly reported in sketches of ambazone) is present in only one structure (RAGNAQ)[14] in the CSD, whereas the disposition of the hydrogen atoms in the tautomeric conformation B is present in nine structures (AZGIY, HAJFIP, MAXYOZ,[15] MAXYUF,[15] MENMEY,[16] NTRGUA,[17] RAGNEU,[14] TANPEE,[18] WASPIP[19]). The C–N distances observed in the structures of ambazone monohydrate (AMB·H_2O) and ambazone anhydrous forms (AMB) are comparable with the ones reported for the tautomeric disposition B and this conformation is adopted in this paper. A total of six salts of ambazone have been reported in literature,[20–25] but no crystal structure is reported so far.

In this article, we present the first crystal structures of the monohydrate and anhydrous forms of ambazone together with their characterization and relative stability investigation. Also, we report a novel acetate salt solvate form of ambazone [AMBAc]·HAc and its potential use in an oral drug product.

EXPERIMENTAL

Materials

The API ambazone monohydrate was purchased from Microsin S.A. (Bucharest, Romania) and was used without further purification. Acetic acid glacial and all other chemicals were supplied by Sigma-Aldrich (Bucharest, Romania) and were of reagent grade.

Correspondence to: Lucia Maini (Telephone: +39-051-2099597; Fax: +39-051-2099456; E-mail: l.maini@unibo.it)

This article contains supplementary material available from the authors upon request or via the Internet at http://onlinelibrary.wiley.com/.

Journal of Pharmaceutical Sciences, Vol. 103, 3594–3601 (2014)

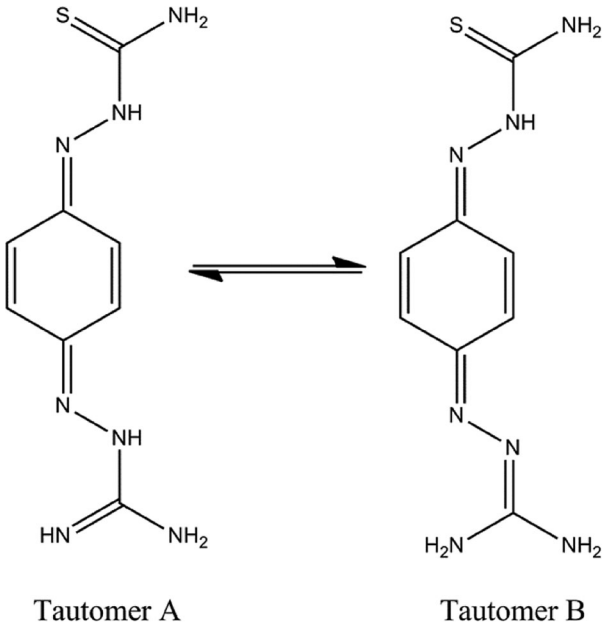

Figure 1. Two chemical structures of the possible tautomers of ambazone ($C_8H_{11}N_7S$).

Crystallization of AMB·H_2O

Plate-like crystals of ambazone monohydrate were grown by diffusion of mixtures of 2 mL pentane and 2 mL diethyl ether in a saturated solution (2 mL) of ambazone in acetone for 5 days at room temperature.

Crystallization of AMB

The anhydrous solid form of ambazone was obtained by heating the monohydrate form at 140°C for 30 min, followed by slow cooling up to 25°C.

A saturated solution (2 mL) of ambazone with *p*-aminobenzoic acid (1:1) molar ration in nitromethane was allowed to diffuse at room temperature in 2 mL tetrahydrofuran and 2 mL hexane. After 5 days, plate-like crystals of anhydrous ambazone were formed.

Crystallization of [AMBAc]·HAc

The novel acetate salt solvate form of ambazone was obtained by placing a glass sample holder, containing the 255 mg powder of ambazone, in a cylindrical weighing bottle containing 10 mL of glacial acetic acid; the reaction took place by vapor diffusion in a closed system at room temperature for 32 h.

Plate-like single crystals of acetate salt solvate form were obtained by vapor diffusion crystallization: a saturated solution of ambazone monohydrate with glacial acetic acid (2 mL) and dichloromethane (2 mL) was exposed to 10 mL diethyl ether vapors for 5 days.

Single-Crystal X-ray Diffraction

Diffraction data for all solid forms were collected using an Oxford XCalibur S Diffractometer (Agilent Technologies, formerly Oxford Diffraction, Oxford, UK) equipped with a graphite monochromator (Mo–Kα radiation, $\lambda = 0.71073$ Å), and a CCD Sapphire detector and Oxford Cryosystem system for data collection at low temperatures. The tube voltage was 50 kV and the maximum current was 40 mA. The data obtained were processed using CrysAlis software. SHELX 97 was used for structure solution and refinement.[26] Nonhydrogen atoms were refined anisotropically. Hydrogen atoms bound to carbon and nitrogen atoms were added at the calculated positions. Hydrogen atoms bound to oxygen atoms were located from a Fourier map and their position refined.

X-ray Powder Diffraction

Powder data were collected on a PANanalytical X'Pert Pro Diffractometer (PANalytical, Almelo, The Netherlands) with Cu $K\alpha_1$ ($\lambda = 1.5406$ Å) and $K\alpha_2$ ($\lambda = 1.5444$ Å) radiation equipped with an X'Celerator detector and a TTK 450 Anton Paar variable temperature camera. The samples were mildly preground in an agate mortar in order to control crystals size and to minimize the preferred orientation effects. The samples were placed in flat sample holder and were scanned from 3° to 40° 2θ at a step size of 0.017°. The Mercury CSD 2.0 program was used for calculation of X-ray powder patterns on the basis of single-crystal data.[27] By comparing the calculated and observed powder diffraction patterns, the correspondence between the bulk materials and the single-crystal structure was obtained.

Differential Scanning Calorimetry

The differential scanning calorimetry (DSC) experiments were carried out on a Shimadzu DSC-60 differential scanning calorimeter (Shimadzu Corporation, Japan) andShimadzu TA-WS60 and TA60 2.1 software were employed for data acquisition and analysis. Nonhermetic crimped aluminum pans, in which 1–2 mg of sample was accurately weighed, were used to perform the experiments. The samples were heated from room temperature up to 350°C under flowing nitrogen flux, the heating rate being 10°C min^{-1}.

Differential Thermal Analysis and Thermogravimetric Analysis

Differential thermal analysis and thermogravimetric analysis (DTA–TGA) measurements were performed with a simultaneous Shimadzu DTG-60/60H apparatus (Shimadzu Corporation, Japan) in the range of 30°C–400°C. Heating was performed in a nitrogen flow (70 cm^3 min^{-1}) using an alumina sample cell (θ, 5.8 × 2.5 mm^2) at the rate of 5 °C min^{-1} up to decomposition. The sample weights were in the range of 5−10 mg. For data collection and analysis, the Shimadzu TA-60WS software was used.

Powder Dissolution Experiments

μDISS Profiler™ apparatus (pION Inc., MA, USA) was used to assess the dissolution rate and the apparent solubility of AMB·H_2O, AMB, and [AMBAc]·HAc. The system consists of an integrated diode array spectrophotometer connected to a fiber optic UV probe located directly in the reaction vessel and measures the concentration as a function of time, without filtering the solution. Measurement of dissolution kinetics and equilibrium solubility was carried out at 450 nm and the concentrations of AMB·H_2O, AMB, and [AMBAc]·HAc were calculated by means of a standard curve. In a typical experiment, 10 mL of deionized water (pH 5.8), physiological serum (pH 6.8), or phosphate buffer (pH 7.0) were added to a flask containing ~1 mg of sample, and the resulting mixture was stirred at 25°C and 400 rpm.

FTIR

All spectra were obtained with a JASCO 6100 FTIR spectrometer (Jasco Inc., MD, USA), and Spectra Manager software was used for data collection. The spectra were recorded in the 400–4000 cm^{-1} spectral domain with a resolution of 4 cm^{-1} and 256 scans. A background spectrum of the potassium bromide pellet was recorded under the same instrumental conditions and subtracted from each sample spectrum. Each sample in pellet was prepared with approximately 1 mg of solid sample mixed with 150 mg of dry pure spectral potassium bromide powder. Data analysis was performed using spectra analysis software.

RESULTS AND DISCUSION

Crystallographic Study

Ambazone monohydrate crystallizes as orange plates, which show twinning by merohedry. The cell parameters are a = 7.2084(3) Å, b = 7.2606(3) Å, c = 22.4102(8) Å, and β = 90.021(4)°, which mimic an orthorhombic cell. The structure was solved as monoclinic $P2_1/c$ with twinning matrix of (1 –0 0, 0 –1 0, 0 0 1).

Crystals of AMB are characterized by nonmerohedric twinning, which was resolved during the data reduction. The anhydrous form crystallizes in the monoclinic space group $P2_1$, with two ambazone molecules in the asymmetric unit (Table 1).

Almost the same conformation of the ambazone molecules is maintained in the two crystal structures as observed by overlaying the molecules with Mercury CSD 2.0.[27]

Ambazone molecules in the asymmetric unit of the anhydrate have similar conformations, with small differences in the terminal primary amino groups (Supplementary Fig. S1a). Slightly higher conformational similarity is found when comparing the ambazone molecule in AMB·H_2O and [AMBAc]·HAc (described further) with one ambazone molecule from the asymmetric unit of the anhydrous form (Supplementary Table S1 and Fig. S1). Therefore, although small, the conformational differences between the two ambazone molecules from the

Table 1. Crystal Data and Details of Measurements

Compound	AMB·H_2O	AMB	[AMBAc]·HAc
Formula	$C_8H_{13}N_7O_1S_1$	$C_8H_{11}N_7S_1$	$C_{12}H_{18}N_7O_4S_1$
Molecular weight ($g \cdot mol^{-1}$)	255.31	237.3	356.39
Temperature (K)	293	293	100
Crystal system	Monoclinic	Monoclinic	Monoclinic
Space group	$P\,2_1/c$	$P\,2_1$	$C\,2/c$
a (Å)	7.2084(3)	7.8470(10)	19.1681(16)
b (Å)	7.2606(3)	17.856(2)	9.3693(17)
c (Å)	22.4102(8)	8.365(2)	17.976(3)
α (°)	90	90	90
β (°)	90.021(4)	109.45(2)	93.998(8)
γ (°)	90	90	90
V ($Å^3$)	1172.89(8)	1105.2(3)	3220.4(8)
Z	4	4	8
F(000)	536	496	1496
μ (Mo–Kα) (mm^{-1})	0.273	0.278	0.236
Calculated density (g/cm^3)	1.446	1.426	1.470
θ range (°)	2.73–29.25	2.58–29.43	3.22–28.79
Measured reflections	17,379	7471	2189
Refined parameters	163	278	128
GOF on F^2	1.116	1.106	1.112
$R1$ [on F, $I>2\sigma(I)$]	0.044	0.106	0.087
w$R2$ (on F^2, all data)	0.097	0.33	0.20

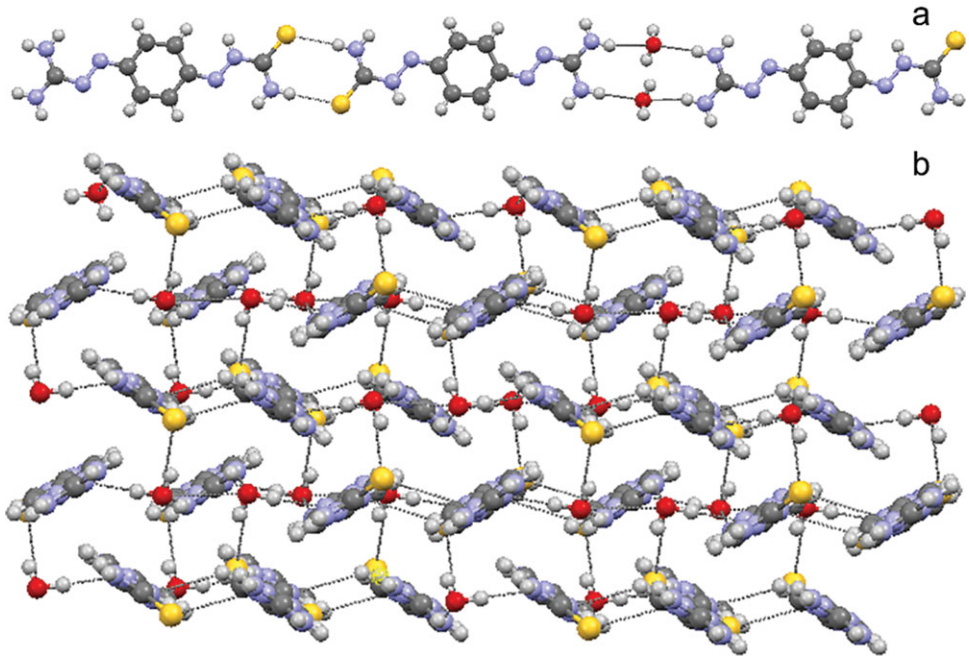

Figure 2. Structure of AMB·H_2O: (a) Hydrogen bond patterns that form the infinite chains. Water molecules are placed over and under the chain. (b) Overall packing with the chains packed in a fishbone fashion.

 DOI 10.1002/jps.24151

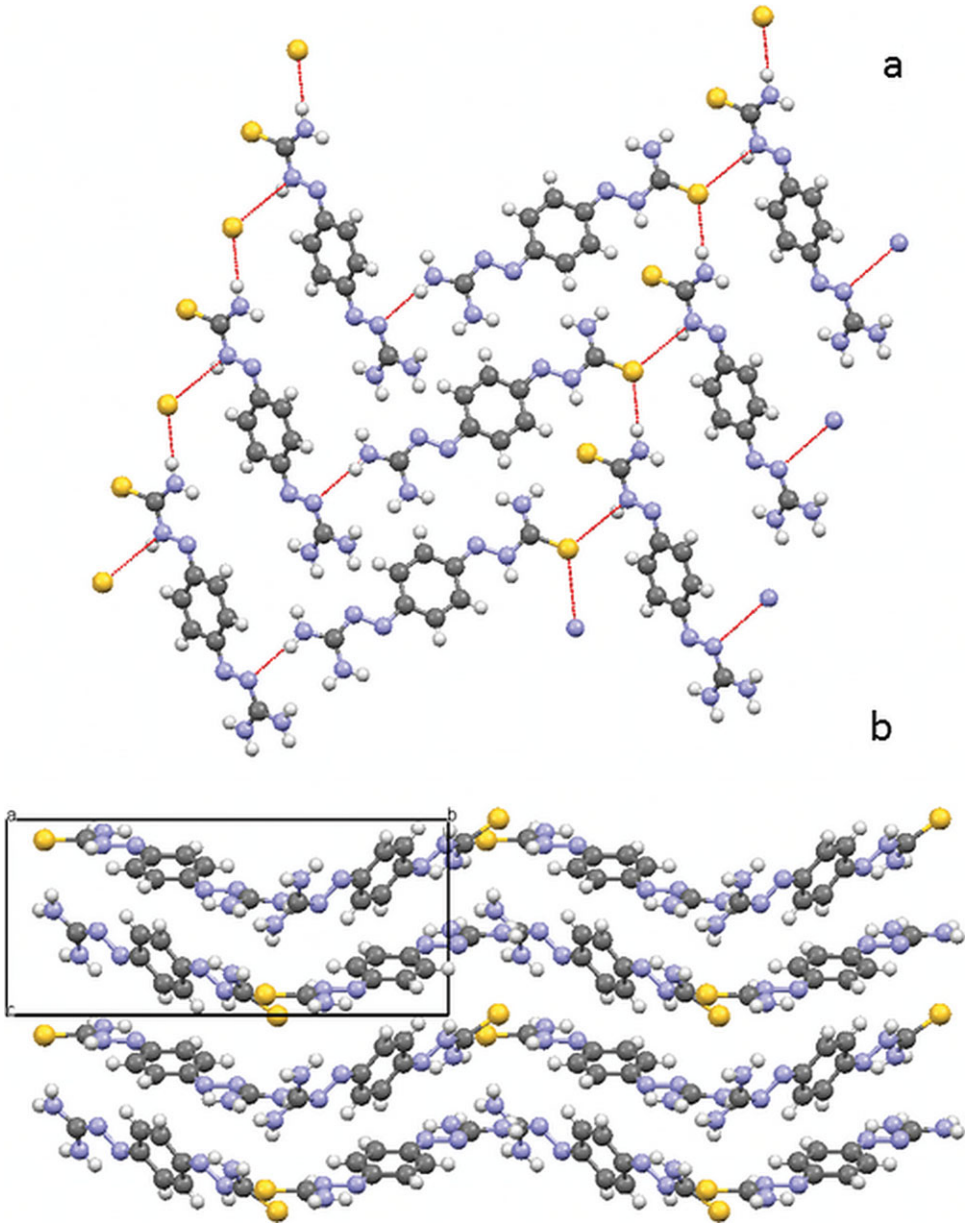

Figure 3. (a) Two-dimensional network of AMB. (b) Crystal packing viewed down *a*-axis. H atoms are excluded for clarity.

asymmetric unit of AMB structure seem sufficient for leading to different conformers.

Important hydrogen bonds in the AMB·H_2O, AMB, and [AMBAc]·HAc crystal structures are shown in Supplementary Table S2.

In the crystal structure of AMB·H_2O, the thiourea groups of ambazone are involved in N–H–S hydrogen bonds and form a R2,2(8) pattern, whereas the diaminomethylidene groups form a ring with the water molecules [R2,4(12)] to obtain infinite flat chains of ambazone (Fig. 2a). These chains are packed in a fishbone fashion, which promotes the C–H π interactions, whereas the water molecules interact with the surrounding chains to form a three-dimensional network (Fig. 2b).

Anhydrous crystal structure AMB presents a different hydrogen bond pattern. The thiourea groups face each other and via lateral hydrogen bonds form an infinite chain involving in a sequence: the nitrogen of the amino group, the sulfur atom, the nitrogen of the hydrazine group, and the sulfur atom (Fig. 3a). The sulfur atom, which is not involved in hydrogen bonds, is surrounded by nitrogen atoms carrying hydrogen pointing toward the S atom. Also, the diamino groups face each other and via multiple hydrogen bonds form a two-dimensional (2D) network. These corrugated planes are staked parallel to each other along the *c*-axis (Fig. 3b).

The presence of the crystal structures of AMB·H_2O and AMB in the corresponding bulk materials was assessed qualitatively by comparing the calculated and experimental X-ray powder diffraction (XRPD) patterns (Supplementary Fig. S2).

[AMBAc]·HAc crystallized in very thin orange prismatic plates, had low diffraction power, and showed a high propensity to form twins. The crystal structure was determined by collecting data at low temperature (100 K). Crystal structure

determination showed a (1:1) acetate salt, plus a neutral acetic acid moiety to make a solvate salt (since the acetic acid is liquid at room temperature). In [AMBAc]·HAc, the coformer is present as anion and as neutral molecule; the proton transfer between ambazone and the acetic acid was assessed by crystallographic data and it was confirmed by FTIR analyses (see Supplementary Information). The presence of the coformer as acid and conjugated base recalls the salt cocrystals where the active ingredient is present as acid and conjugated base.[28,29] The ionization state of [AMBAc]·HAc is in line with the ΔpKa of 5.93 between the strongest basic site of ambazone ($pKa = 10.69$) and acetic acid ($pKa = 4.75$). On the basis of ΔpKa rule proposed by Childs et al.,[4] the other two basic sites of ambazone with $pKa = 7.39$ and 6.22 are not strong enough (?pKa with respect to acetic acid < 3) to generate further ionization with acetic acid and therefore the formation of a solvate is preferred.

The ambazone molecule is rich in donating hydrogen bond groups and is surrounded by the acetic and acetate molecules, which are rich in accepting hydrogen bonds. The ambazone forms a strong hydrogen bond with the acetic acid, and the multiple hydrogen bonds between the acetic acid, acetate, and ambazone form a three-dimensional (3D) network as shown in Figure 4. The crystal structure is also stabilized by the formation of π–π stacking between the ambazone molecules.

The presence of [AMBAc]·HAc determined the crystal structure in the corresponding bulk sample, which was qualitatively assessed by XRPD (Supplementary Fig. S3). The differences between the experimental and calculated XRPD patterns are related to the temperature difference between the single-crystal and the powder diffraction measurements.

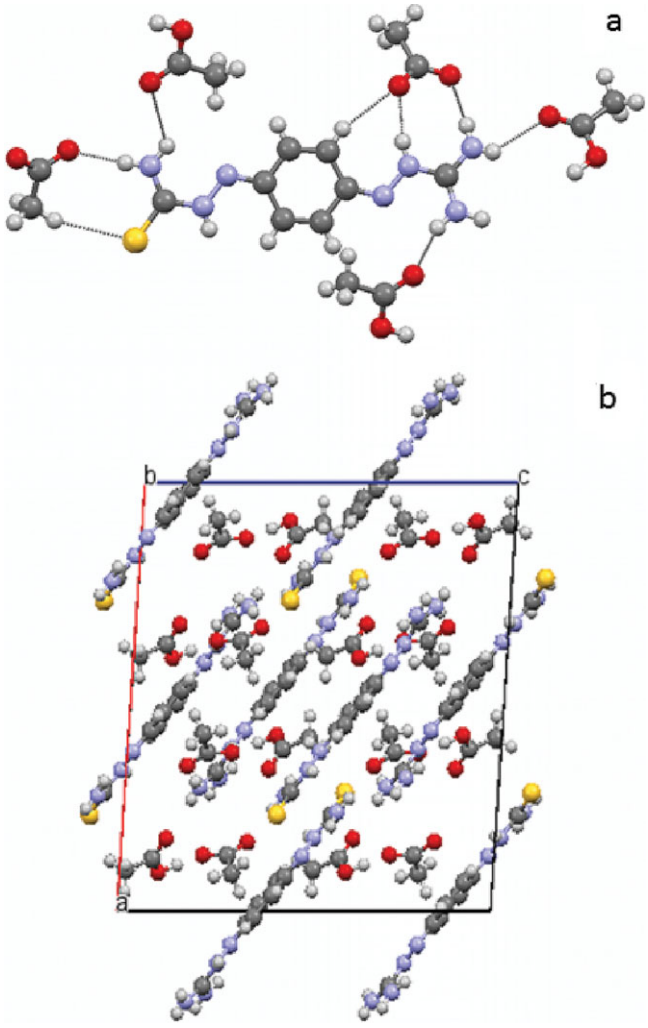

Figure 4. (a) Ambazone acetate salt solvate crystal structure [AMBAc]·HAc. (b) Crystal packing.

Thermodynamic Study

The thermal behavior of monohydrate, anhydrous, and acetate salt solvate of ambazone forms was studied by simultaneously DTA–TGA and DSC analyses.[30,31] The DTA–TGA and DSC traces obtained for each sample are shown in Figures 5a–5d.

The DSC and DTA curves of AMB·H_2O revealed a broad endothermic signal from 100°C to 150°C, with a maximum at ~133°C that corresponds to the release of the water molecule as confirmed by the 6.93% weight loss detected in the TGA (calculated 7.05%) (Figs. 5a and 5d).

At higher temperature, the DTA and DSC curves are characterized by a sharp exothermic peak, which corresponds to a weight loss of 8.4% in the TGA. Ambazone decomposes at 210°C before melting. As expected, DSC and DTA traces for AMB show only the sharp exothermic signal at ~200°C attributed to ambazone degradation. No weight loss is detected in the TGA up to the degradation process (Fig. 5b). The DSC/DTA curve of [AMBAc]·HAc presents the endothermic event with a maximum at 156.8°C, followed by two exothermic events. The endothermic event corresponds to the loss of one acetic acid molecule with a 16.9% total weight loss in the TGA (calculated 16.8%), which is suddenly followed by the release of the second acetic acid molecule and degradation of the ambazone (Figs. 5c and 5d).

The dehydration process of AMB·H_2O was further investigated by temperature-dependent XRPD. The loss of the water molecules is observed at 110°C when a mixture of AMB·H_2O and AMB is obtained. The dehydration process is completed at 140°C and the powder pattern is consistent with AMB. Upon further heating, the anhydrous form remains stable up to 198°C after which the ambazone degrades and transforms in amorphous (Supplementary Fig. S4). The reverse hydration process of ambazone was evidenced via accelerated stability testing on storage at 40°C/75% relative humidity (RH) of anhydrous form, when complete hydration of ambazone into AMB·H_2O occurred within 60 days. The hydration process takes only few minutes by grinding anhydrous form AMB in the presence of one drop of water in a mortar (Supplementary Fig. S5).

In the case of [AMBAc]·HAc, the heating treatment in the 100–140°C temperature range for 30 min followed by XRPD analysis gave insight into the thermal stability of the solid form. The results are in agreement with the thermal analysis data showing the onset of the acetic acid loss at about 140°C. Further temperature increase to 150°C showed the presence of the amorphous phase, indicating that the crystal structure degrades upon the loss of acetic acid (Supplementary Fig. S6). Further stability testing of [AMBAc]·HAc on storage at 40°C/75% RH showed transformation into the monohydrate within 5 days (Supplementary Fig. S7).

 DOI 10.1002/jps.24151

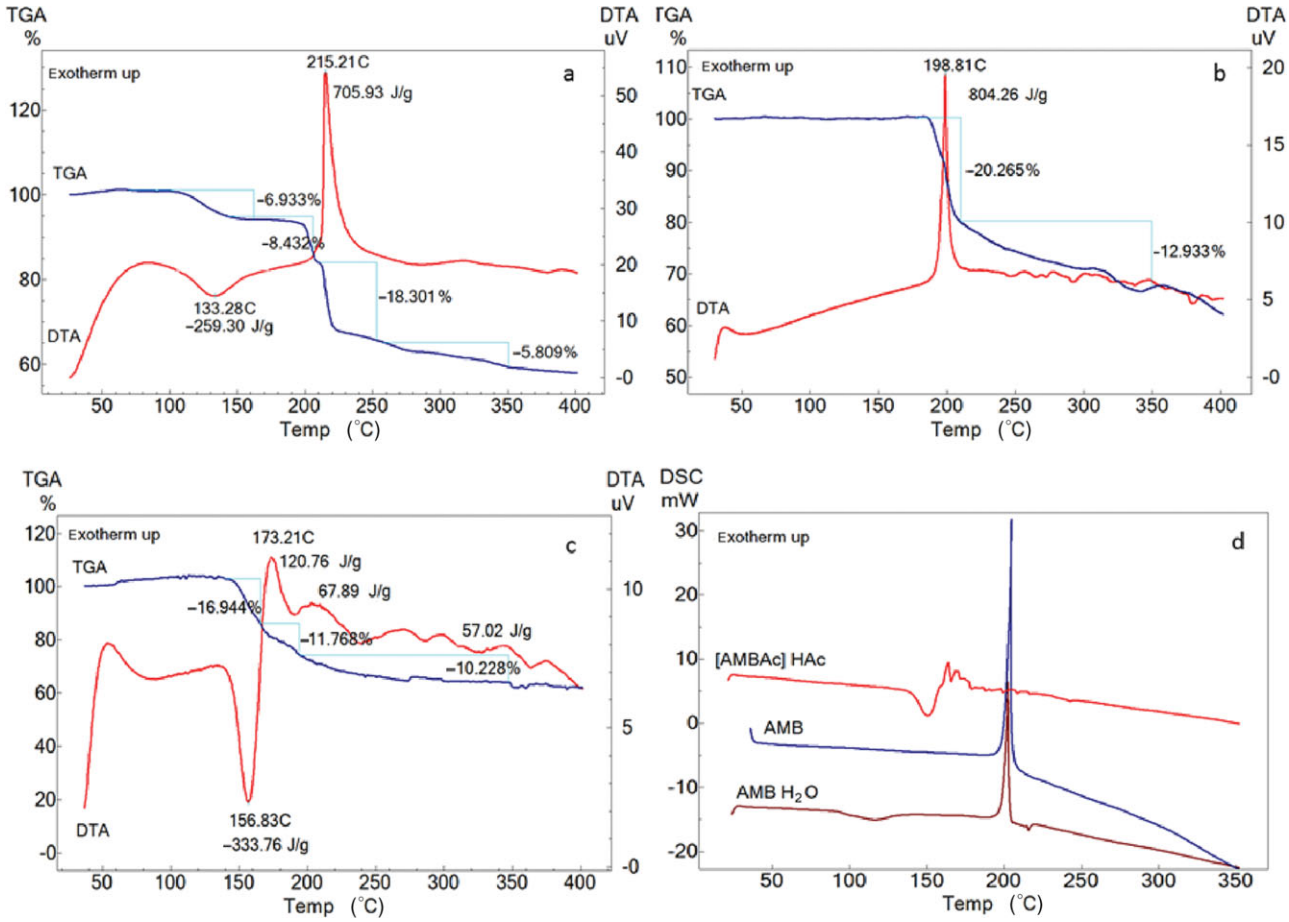

Figure 5. DTA–TGA curves of (a) AMB·H_2O; (b) AMB; (c) [AMBAc]·HAc; and (d) DSC curves of AMB·H_2O, AMB, and [AMBAc]·HAc.

Powder Dissolution Testing

Dissolution profiles of the studied solid forms in water, physiological serum, and phosphate buffer are shown in Figures 6a–6c.

For [AMBAc]·HAc, the powder dissolution measurements revealed a faster dissolution rate compared with AMB·H_2O and AMB. In water, the dissolution rate of the acetate salt solvate was almost instantaneous and the aqueous solubility was found to be at least six times higher than of the monohydrate and anhydrous ambazone.

Because of the UV signal saturation in the case of ambazone acetate solvate-salt, solubility assessment was carried out by visual inspection after the addition of small volumes of water to a known amount of powder materials. In this way, [AMBAc]·HAc had a water solubility of about 6.5 mg/mL compared with the <1 mg/mL reported solubility in the case of AMB·H_2O.[12] After the dissolution experiments in water, the undissolved solids of monohydrate and anhydrous ambazone were filtered, air-dried, and the solid form stability was confirmed by XRPD analyses (Supplementary Fig. S8). The anhydrous form AMB easily converts into the monohydrate, the transformation being visible during the dissolution experiment (peak in the anhydrate dissolution curve at approximately 3 min) and confirmed by XRPD at the end of the dissolution experiment. For ambazone acetate salt solvate [AMBAc]·HAc, a clear solution of pH ~5 was maintained during the dissolution experiment, indicating its stability against precipitation in water. The dissolution experiments in physiologic serum containing NaCl and pH 7.0 phosphate buffer showed a clear improvement in the dissolution rate and solubility of the acetate salt solvate compared with the solid forms of ambazone. Also in these cases, no precipitation of the acetate salt solvate was observed during the measurements, indicating the solution stability of the form in relevant physiological media.

CONCLUSIONS

We have presented here the first crystal structures of ambazone, one of the oldest and widely used antimicrobial pharmaceutical ingredient. Crystal structures of AMB·H_2O and AMB were determined by single-crystal X-ray diffraction (SC-XRD) and showed the role of the water molecule in the formation of an infinite 3D network, whereas a 2D network is present in the anhydrous form. Thermal analysis, temperature-dependent XRPD, and accelerated stability testing on storage at elevated temperature and RH evidenced the reversible transformation between the monohydrate and the anhydrous forms (Fig. 7).

This study also shows the ability of ambazone to form a salt solvate with acetic acid with a (1:1:1) stoichiometry, its nature being identified from structure solution by SC-XRD. [AMBAc]·HAc has substantially higher aqueous solubility and

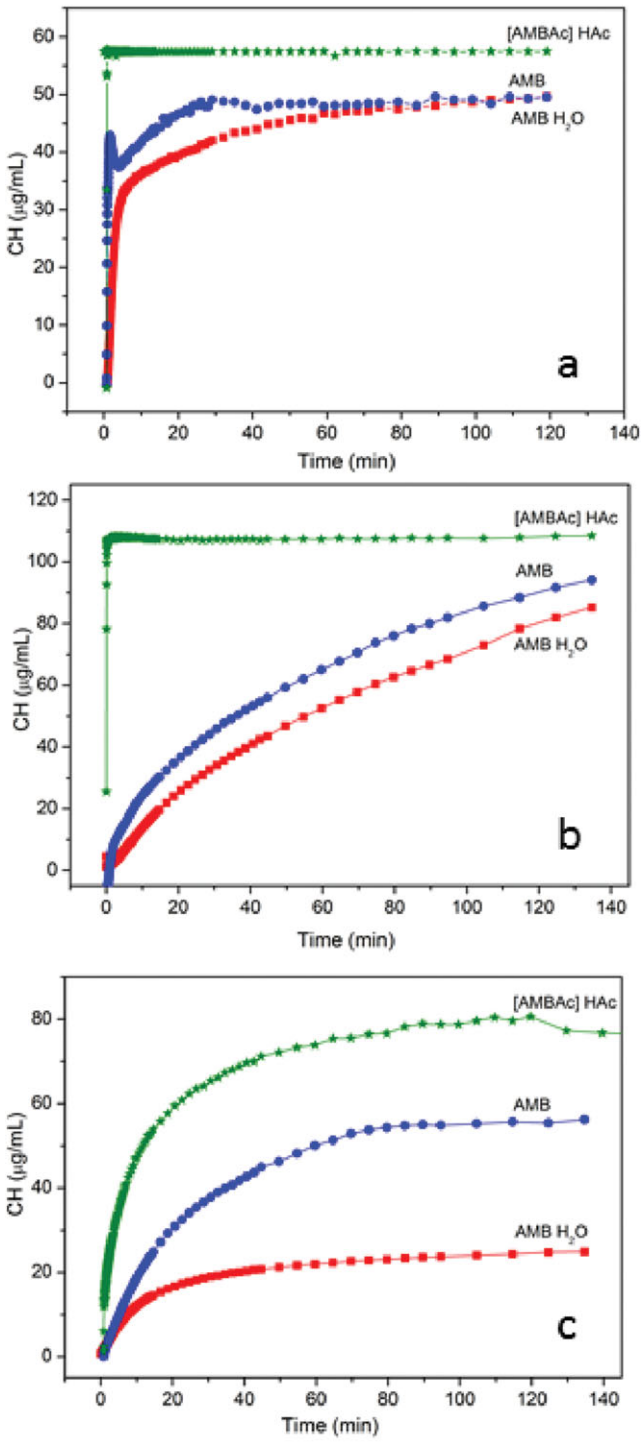

Figure 6. Dissolution profiles at different aqueous medium (µg/mL vs. minute): (a) Deionized water (pH 5.81), (b) physiologic serum (pH 6.8), and (c) phosphate buffer (pH 7.0).

dissolution rate than the solid forms of ambazone, and it is thermally stable in solid state up to 140°C but it transforms to ambazone monohydrate on storage at elevated temperature and RH.

The results show the potential of the acetate salt solvated form of ambazone to be developed in an oral formulation with improved solubility and bioavailability compared with the poorly water-soluble ambazone. The instability of the salt solvate at elevated temperature and RH represents a development risk that could be mitigated by a careful control of the storage conditions.

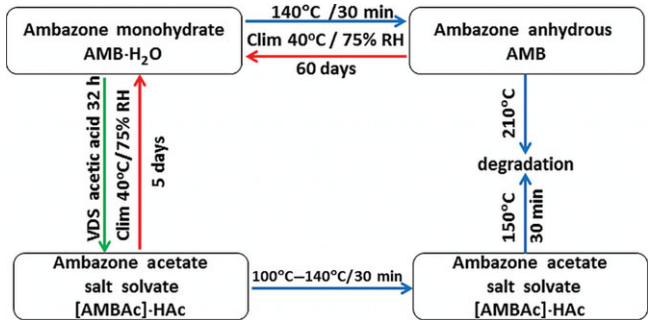

Figure 7. Stability relationships between the ambazone monohydrate, anhydrous, and the acetate salt solvate forms reported in this study.

ACKNOWLEDGMENTS

This study was supported by ANCS project POSCCE ID536. The authors thank University of Bologna for a postdoctoral stage at the Dipartimento di Chimica G Ciamician.

REFERENCES

1. Brittain HG. 2009. Polymorphism in pharmaceutical solids. Vol. 192. 2nd ed. New York: Informa Healthcare Press, pp 120–124.
2. Sekhon BS. 2009. Pharmaceutical co-crystals —A review. Ars Pharm 50:99–117.
3. Braga D, Grepioni F, Maini L, Polito M. 2009. Crystal polymorphism and multiple crystal forms. Struct Bond 132:25–50.
4. Childs S L, Stahly GP, Park A. 2007. The salt-cocrystal continuum: The influence of crystal structure on ionization state. Mol Pharm 4:323–338.
5. Fulga I, Negut M, Nascutiu AM, Nemet C, Toma F, Grigore L, Nitescu R, Marcu C, Nedelcu L, Spircu T. 2007. Microbial sensitivity to ambazone (Faringosept) in pharyngeal samples from patients with acute infections of the upper respiratory tract. Bacteriol Virusol Parazitol Epidemiol 52(1–2):19–27.
6. Manimaran A, Jayabalakrishnan C. 2012. DNA-binding, catalytic oxidation, CAC coupling reactions and antibacterial activities of binuclear Ru(II) thiosemicarbazone complexes: Synthesis and spectral characterization. J Adv Res 3(3):233–243.
7. Amlacher R, Baumgart J, Hart A, Weber H, Kühnel J, Schulze W, Hoffmann H. 1990. Influence of age on antileukemic action, subacute toxicity and tissue distribution of ambazone in B6D2F1 mice. Arch Geschwulstforsch 60(1):11–18.
8. Amlacher R, Kühnel HJ, Niemann G, Schulze W. 1986. Pharmacokinetics of ^{14}C–ambazone (1,4-benzochinone–guanylhydrazone–^{14}C–thiosemicarbazone) in B6D2F1 mice. Pharmazie 41(2):155.
9. Amlacher R, Mackowiak A, Baumgart J, Schulze W, Hoffmann H. 1990. Influence of murine melanoma B16 on the distribution of ambazone in B6D2F1 mice. Pharmazie 45(5):379–380.
10. Kühnel HJ, Amlacher R, Baumgart J, Schulze W. 1988. Distribution of 14C-ambazone in normal and leukemia P 388-bearing mice. Arch Geschwulstforsch 58(4):217–222.
11. Gutsche W, Hartl A, Baumgart J, Schulze W. 1990. Antineoplastic activity and toxicity of dihydroambazone in comparison with ambazone (1,4-benzoquinone guanylhydrazonethiosemi-carbazone). Pharmazie 45(1):55–57.

12. Löber G, Hoffmann H. 1990. Ambazone as a membrane active antitumor drug. Biophys Chem 35(2–3):287–300.
13. Andreani A, Rambaldi M, Locatelli A, Bossa R, Fraccari A, Galatulas I. 1992. Potential antitumor agents. 21. Structure determination and antitumor activity of imidazo[2,1-b]thiazole guanylhydrazones. J Med Chem 35(24):4634–4637.
14. Medvedeva MI, Tugusheva NZ, Alekseeva LM, Kalinkina MA, Parshin VA, Chernyshev VV, Levina VI, Grigor'ev NB, Shashkov AS, Granik VG. 2010. Reactions of aminoguanidine and guanidine with 3- and 5-formyl-4-arylaminopyridones. Izv Akad Nauk SSSR, SerKhim (Russ) (RussChemBull) 59(12):2247–2258.
15. Györgydeák Z, Holzer W, Mereiter K. 1999. Guanylhydrazones of (hetero) aryl methyl ketones: Structure and reaction with acetic anhydride. Monatsh Chem 130(7):899–913.
16. Demir S, Dinçer M, Saripinar E. 2006. 2-(1-Phenylethylideneamino) guanidine. Acta Cryst Sect E Struct Rep Online 62(9):4194–4195.
17. Bryden JH, Burkhardt LA, Hughes EW, Donohue J. 1956. The crystal structure of nitroguanidine. Acta Crystallogr 9(7):573–578.
18. Murmann RK, Glaser R, Barnes CL. 2005. Structures of nitroso- and nitroguanidine X-ray crystallography and computational analysis. J Chem Cryst 35(4):317–325.
19. Cousson A, Nectoux F, Bachet B, Kokel B, Hubert-Habart M. 1993. Structure of 5-[1-(diaminomethylenehydrazono) ethyl]- 4-methyl-2-methylthiopyrimidine. Acta Crystallogr Sect C Cryst Struct Commun 49(9):1670–1673.
20. Mureşan-Pop M, Kacso´ I, Tripon C, Moldovan Z, Borodi G, Bratu I, Simon S. 2011. Spectroscopic and structural study of the ambazone hydrochloride. J Therm Anal Calorim 104(1):299–306.
21. Mureşan-Pop M, Kacsó I, Filip X, Vanea E, Borodi G, Leopold N, Bratu I, Simon S. 2011. Spectroscopic and physical–chemical characterization of ambazone–glutamate salt. Spectroscopy 26(2):115–128.
22. Kacsó I, Racz C, Santa S, Rus L, Dadarlat D, Borodi G, Bratu I. 2012. Ambazone–lipoic acid salt: Structural and thermal characterization. Thermochim Acta 550:13–18.
23. Kacsó I, Rus L, Pop M, Borodi G, Bratu I. 2012. Structural characterization of ambazone salt with niflumic acid. Spectroscopy 27(1):49–58.
24. Borodi G, Mureşan-Pop M, Kacsó I, Bratu I. 2012. Structural investigation of ambazone with lactic acid. AIP Conf Proc 1425:9–12.
25. Kacso I, Mureşan-Pop M, Borodi G, Bratu I. 2012. Structural characterization of ambazone salt with nicotinic acid. AIP Conf Proc 1425:30–34.
26. Sheldrick GM. 1997. SHELXL-97: Program for the refinement of crystal structures. Göttingen, Germany: University of Göttingen.
27. Macrae CF, Bruno IJ, Chisholm JA, Edgington PR, McCabe P, Pidcock E, Rodriguez-Monge L, Taylor R, van de Streek J, Wood PA. 2008. Mercury CSD 2.0—New features for the visualization and investigation of crystal structures. J Appl Cryst 41(2):466–470.
28. Pop MM, Sieger P, Cains PW. 2009. Tiotropium fumarate: An interesting pharmaceutical co-crystal. J Pharm Sci 98(5):1820–1834.
29. Chierotti MR, Gaglioti K, Gobetto R, Braga D, Grepioni F, Maini L. 2013. From molecular crystals to salt co-crystals of barbituric acid via the carbonate ion and an improvement of the solid state properties. CrystEngComm 15:7598–7605.
30. Giron D. 1995. Thermal analysis and calorimetric methods in the characterisation of polymorphs and solvates. Thermochim Acta 248:1–59.
31. Giron D, Mutz M, Garnier S. 2004. Solid-state of pharmaceutical compounds. Impact of the ICH Q6 guideline on industrial development. J Therm Anal Calorim 77(2):709–747.